

Occurrence of ferromagnetic shape memory alloys (invited)

Manfred Wuttig, Luohong Liu, Koichi Tsuchiya, and Richard D. James

Citation: *J. Appl. Phys.* **87**, 4707 (2000); doi: 10.1063/1.373135

View online: <http://dx.doi.org/10.1063/1.373135>

View Table of Contents: <http://jap.aip.org/resource/1/JAPIAU/v87/i9>

Published by the [AIP Publishing LLC](#).

Additional information on *J. Appl. Phys.*

Journal Homepage: <http://jap.aip.org/>

Journal Information: http://jap.aip.org/about/about_the_journal

Top downloads: http://jap.aip.org/features/most_downloaded

Information for Authors: <http://jap.aip.org/authors>

ADVERTISEMENT



**Running in Circles Looking
for the Best Science Job?**

Search hundreds of exciting
new jobs each month!

<http://careers.physicstoday.org/jobs>

physicstodayJOBS



Occurrence of ferromagnetic shape memory alloys (invited)

Manfred Wuttig and Luohong Liu

Department of Materials Science and Engineering, University of Maryland, College Park, Maryland 20742-2115

Koichi Tsuchiya

Department of Production Systems Engineering, Toyohashi University of Technology, Toyahashi, Aichi, 441-8580 Japan

Richard D. James

Department of Aerospace Engineering and Mechanics, University of Minnesota, Minneapolis, Minnesota 55455

This article presents an overview of the necessary conditions for the formation of shape memory alloys (SMAs) and how these must overlap with the occurrence of ferromagnetism so that ferromagnetic shape memory alloys (MSMAs) may be formed. The electronic, elastic, and geometric conditions permit an understanding of the occurrence of Cu- and Fe-based SMAs as well as NiMnGa Heusler MSMAs except that the naively determined critical electron concentration for the latter, 7.3, disagrees with the values of 1.5 and 8.6 accepted for the Hume–Rothery phases and certain Fe-based systems. © 2000 American Institute of Physics. [S0021-8979(00)39908-X]

INTRODUCTION

This article presents an overview of the conditions for the occurrence of shape memory alloys (SMAs) and ferromagnetic shape memory alloys (MSMAs), concentrating on Cu- and Fe-based alloys. SMAs are based on martensite which is, usually a nonequilibrium phase which develops when a high-temperature phase is quenched so that the low-temperature equilibrium phase cannot develop. The historical example is Fe–C martensite forming the backbone of steel metallurgy. Martensite often forms at critical electron concentrations. The product phases can be anticipated from a knowledge of the elastic properties of the high-temperature phase at various points in reciprocal space. SMAs form a subclass of martensitically transforming alloys identified by the special geometrical relationships between the parent and product phases. MSMAs, finally, are conceptually the alloys located in the lens-shaped overlap region between the SMAs and ferromagnetic alloys shown in Fig. 1.

MARTENSITE

The fcc Fe–C solid-solution transforms to a bct phase, called “martensite,” if cooled sufficiently quickly so that the diffusion-controlled formation of the equilibrium cementite, Fe₃C, graphite, and bcc Fe–C solid solution is suppressed.¹ The formation and properties of martensite form one of the backbones of the steel industry. The name “martensite” has subsequently been generalized to structural phase transformations which are “shear-dominant lattice distortive and occurring by nucleation and growth,”² i.e., are of first order. As the attendant volume changes and large shear deformations are accommodated by plastic deformation, they are also irreversible. As such, the martensitic transformation is hysteretic, meaning that the forward and reverse transformations start at different temperatures. For Fe–C martensites this hysteresis is, typically, a few hundred degrees. Having been formed by shear, martensite is generally characterized by

acicular microstructures, as shown in Fig. 2. The lenticular shape of some of the dark martensite portions recognizable in the right-hand part of Fig. 2 reduces the shear stresses created by the transformation. This shear stress is large, as can be seen from Fig. 3 by comparing the lattice correspondence and ideal c/a ratio $\sqrt{2}$ of the fcc and bct structures with the observed c/a ratios of Fe–C martensites of the order of 1.1 or less.³

SHAPE MEMORY ALLOYS

Shape memory alloys are alloys which undergo a reversible martensitic transformation. Reversibility can be assured in two ways. First, the transformation can be second order, and second, it can be of first order if the lattice constants of the parent and product structures permit the martensite to grow in the austenite without creating long-range stress fields or excess interfacial energy. Shape memory alloys thus form a subgroup of all alloys undergoing a martensitic transformation, as shown in Fig. 1.

In recent years, the precise conditions on lattice parameters that are associated with a reversible shape memory ef-

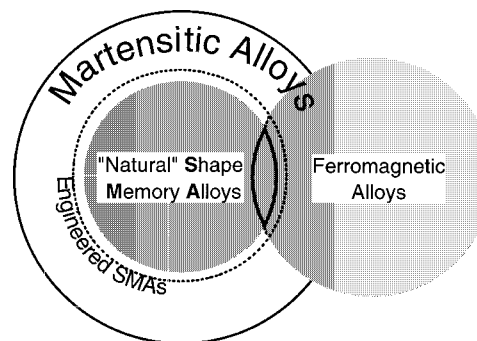


FIG. 1. Schematic presentation of the location of MSMAs in the lens-shaped region formed by the overlap of SMAs and ferromagnetic alloys.

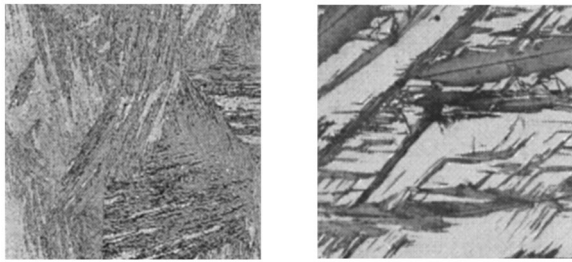


FIG. 2. Typical martensitic microstructures of low (left) and high (right) carbon steels. Note that the microstructures have an irregular character.

fect have been established. For additional information and references, see the review article, Ref. 4. The origins of such conditions are the following: The free-energy densities of martensitic materials have a certain number n [= (order of the point group of the austenite)/(order of the point group of martensite)] of energy wells. These are defined by special strains $\epsilon_1, \dots, \epsilon_n$. These strains ϵ_i are determined by the lattice parameters of the relaxed austenite and martensite phases. Under certain very special conditions on lattice parameters, certain low-energy microstructures become possible that promote the shape memory effect. The known conditions are of two types:

(a) Special lattice parameters that allow additional “rank-one connections” between energy wells (or between the states that are achievable by mixing strains from the energy wells). The rank-one connections imply the existence of a large class of energy minimizing martensitic microstructures that give great flexibility to change volume fractions of the martensite.

(b) Special lattice parameters that allow exact compatibility between austenite and martensite, therefore, eliminating the necessity of overcoming the bulk energy stored in the transition layer’s austenite/martensite interfaces.

These conditions imply low hysteresis by giving a special low-energy path from austenite to martensite.

There are numerous examples given in Ref. 4, but for the purpose of illustration we mention one of them in category (a) Cu–14.0 wt.%Al–3.5 wt.%Ni is a reversible shape memory alloy that was found by alloying so as to have a reversible shape memory effect and a convenient transformation temperature. It undergoes a cubic-to-orthorhombic (β_1 to γ_1') transformation whose strains are characterized by the three lattice parameters α , β , and γ . It exhibits a microstructure (the “wedge”), shown in Fig. 4, that is characteristic of

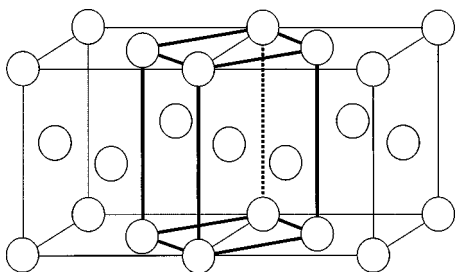


FIG. 3. Structural relationship between the fcc (light lines) and inscribed bcc (dark lines) phases.

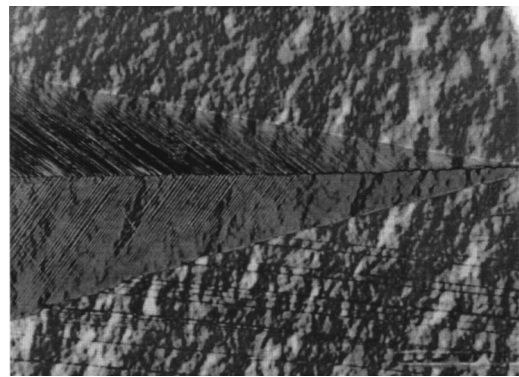


FIG. 4. Wedge-type martensitic microstructure in a CuNiAl alloy.

several shape memory materials. The wedge is only possible as an energy minimizing microstructure with special lattice parameters. These are illustrated in Fig. 5. For the purpose of this illustration, the three lattice parameters have been reduced to two by putting $\beta=0.9178$, the measured value for this alloy. Under this restriction, the remaining lattice parameters α and γ that permit the wedge are given as the dashed (wedged made with type-II twins) or solid (wedged made with type-I twins) lines. The measured lattice parameters α and γ for Cu–14.0 wt.%Al–3.5 wt.%Ni are shown as the small dot.

The wedge may seem to be only one rather special microstructure, but the additional rank-one connections between energy wells implied by being on one of the curves in Fig. 5 implies the existence of a host of other hierarchical microstructures that are energy minimizing (many of these are observed in this alloy).

These considerations have interesting implications for Ni_2MnGa . This alloy is known to have small hysteresis and

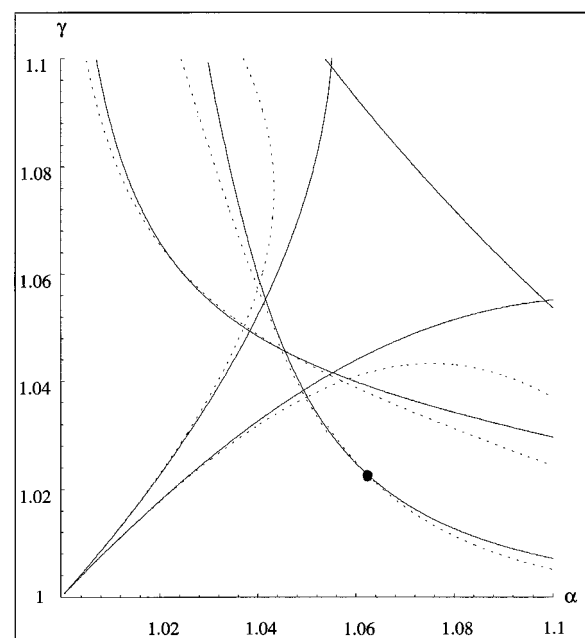


FIG. 5. Wedge accommodation in measured lattice parameters indicated by the solid dot. Note that the wedge is accommodated by both type-I and type-II twins accounting for the small hysteresis in this alloy.

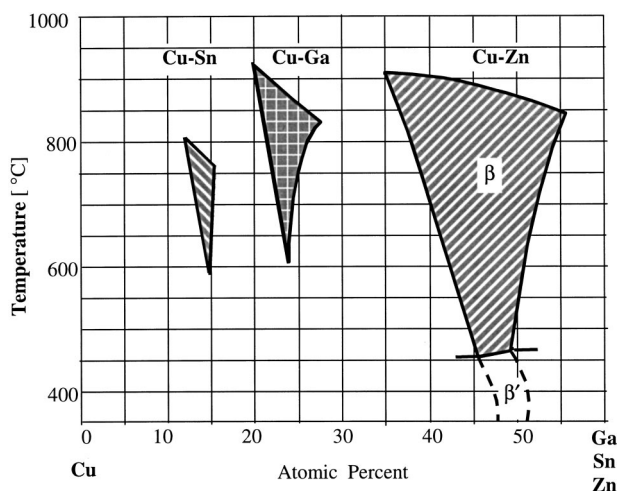


FIG. 6. Ranges of stability of the bcc β phase in CuZn, CuGa, and CuSn alloys. Note that this phase occurs at an electron concentration of approximately 1.5.

an extremely repeatable austenite–martensite phase transformation. For example, M_s and A_s each vary by less than 1 C with cycling for 1–25 cycles, which is much less than is observed in NiTi. So, we seek “special relations” among its lattice parameters. There is nothing remarkable about those of its thermal martensite, and in fact, they imply a relatively large volume change, but there are a number of nearby phases that can be induced by applying small stresses. These include an orthorhombic phase and another tetragonal phase with $c/a > 1$. Remarkably, based on measured lattice parameters, the thermal martensite and the orthorhombic phase satisfy restrictions that imply exact compatibility between them. Furthermore, the orthorhombic and stress-induced tetragonal phase also nearly satisfy these conditions. Thus, it can be summarized that the alloy has a large number (nine) of low-lying energy wells, in addition to the three wells associated with the thermal martensite, and there are certain nongeneric relations between these wells that make for low-energy microstructures. A complete understanding of the relation between these special restrictions and the repeatability of the austenite–martensite transformation in the alloy awaits further study.

There will be alloys which transform martensitically but for which the structural relationships outlined are marginally fulfilled. In that case, the changes of the lattice parameters created by coherent precipitates are sufficiently large so that the above conditions are better met. This philosophy has been successfully applied to FeNiCoTi alloys.⁵

OCCURRENCE OF SMAS

SMAs can be located by inquiring into the driving force of the martensitic transformation. It has long been known that the bcc phase of Hume–Rothery brasses, e.g., CuZn, CuGa, and CuSn alloys, occurs at an s -electron concentration of approximately 1.5, as can be seen from Fig. 6. At high temperatures the bcc phase is stabilized by the vibrational entropy and it will transform by a $[110][110]$ martensitic shear⁶ to the close-packed fcc structure upon cooling/

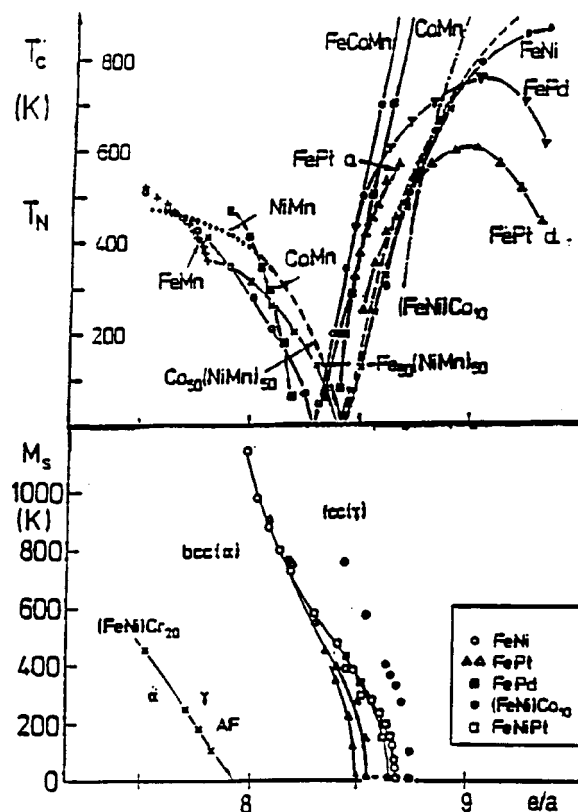


FIG. 7. Ranges of stability of ferro- and antiferromagnetic (top) as well as structural, fcc, and bcc (bottom) phases as a function of the d -electron concentration.

quenching, a conceptually satisfying argument which is also supported by detailed calculations.^{7,8} It would follow that the elastic constants, or certain shear modes at finite wave vectors, e.g.,⁹ decrease upon approaching the martensitic transformation from above. The simplest situation occurs when the martensitic transformation in an alloy is of the second order. In that case, the alloy would be automatically a SMA since the lattice parameters of the high- and low-temperature phases equal each other at the critical temperature. If the transition is fcc–fcc, one would expect that the elastic constant $1/2(C_{11}-C_{12})$ approaches zero at the transition temperature, which is the case in InTi, for example.¹⁰ In the best-known SMA, NiTi, both $1/2(C_{11}-C_{12})$ and C_{44} soften prior to the formation of the monoclinic martensitic phase.¹¹

The martensitic transformation in Fe–Ni alloys is driven by the magnetic d -electron states,¹² as can be appreciated from the striking coincidence of the ferromagnetic–antiferromagnetic and structural stability ranges shown in Fig. 7. First-principle calculations of the energy as a function of the volume and moment¹³ lead to an understanding of why the less dense bcc structure is stable at low temperature in ferrous martensites. Anomalies of the elastic constants are also magnetically driven.¹⁴ Almost complete softening of $1/2(C_{11}-C_{12})$ is observed in FePd.¹⁵

OCCURRENCE OF MSMAs

The foregoing comments indicate the SMAs can be located by considering “electronic” instabilities, elastic soft-

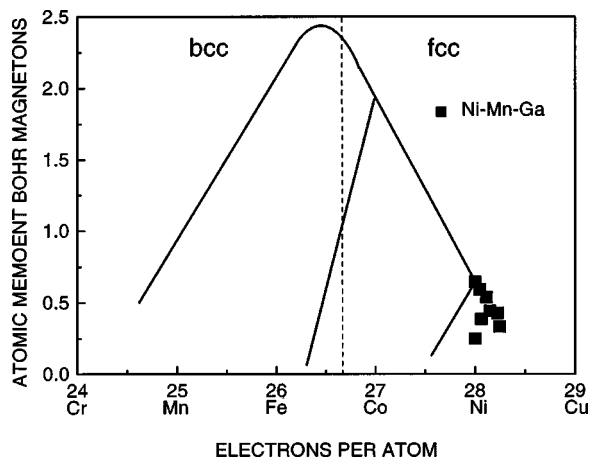


FIG. 8. Schematic Slater–Pauling curve of NiMnGa alloys. The known portions of the curve are indicated schematically only.

ening of the bcc β phase, and the detailed structural relationship between the high- and low-temperature phases. Concentrating on the second and third criteria, one could have, in retrospect, located ferromagnetic Ni_2MnGa Heusler alloys,^{16,17} as the $L1_2$ and bcc structures are closely related, the elastic constants are anomalous¹⁸ and the $1/3[110]TA_2$ phonon softens similar to NiAl.¹⁹ In addition, the high- and low-temperature lattice parameters fit.

NiMnGa MSMAs appear to conform to the known criteria of the occurrence of ferromagnetism in alloys. This can be seen from Fig. 8, showing schematically the known²⁰ Slater–Pauling plot to which NiMnGa magnetization data have been added. Also, the martensitic transition temperatures of known MSMAs can be plotted as a function of the total average ($s+d$) electron concentration. The result is shown in Fig. 9. The data for Fig. 9 have been compiled from various sources.²¹ With the exception of a few data points, which will be discussed below, Fig. 9 clearly shows a critical electron concentration like for Hume–Rothery phases and FeNi alloys. The nonconforming data points pertain to Cu_2MnGa with an unknown M_s temperature above room

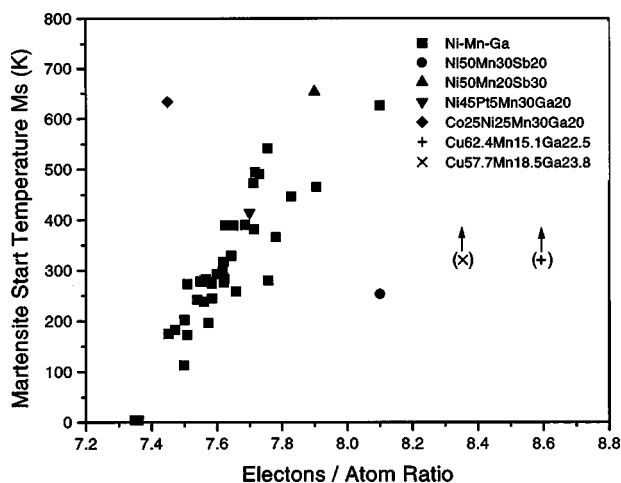


FIG. 9. Martensite start temperatures of known MSMAs as a function of the total average $s+d$ electron concentration.

TABLE I. Compilation of Heusler alloys with electron/atom (e/a) ratios in the range where MSMAs may be found. Known MSMAs are in bold face.

Alloy	Curie temp. (K)	e/a
Co_2MnIn		7
Fe_2MnP		
Co_2MnAl	693	
Co_2MnGa	694	
Ru_2MnSb	$T_n = 200$	
Rh_2MnAl		
Rh_2MnGa		
Rh_2MnIn		
Co_2MnGe		7.25
Co_2MnSn	829	
Rh_2MnGe		
Co_2MnSi	985	
Rh_2MnSn	410	
Rh_2MnPb	355	
Pd_2MnGa		7.5
Ni_2MnGa	379	
Ni_2MnAl	$T_n = 30$	
Co_2MnSb		
Ni_2MnIn	323	
Pt_2MnAl		
Pd_2MnIn	$T_n = 150$	
Rh_2MnSb		
Ni_2MnSn	345	7.75
Pd_2MnGe		
Pd_2MnSn		
Ag_2MnIn		8
Cu_2MnAl	603	
(Ni_2MnSb)	331	
Cu_2MnSn	530	
Pd_2MnAs		
Cu_2MnIn	500	
Au_2MnAl		
Pd_2MnSb	220	
Cu_2MnGa	>RT	
Cu_2MnSb		8.5

temperature (RT),²² a Co and one Sb-containing alloy,²³ both of which have not yet been completely analyzed.

MSMAs can naturally be found in Fe-based alloys and the engineered FeNiCoTi alloys were already mentioned above. FePt alloys are MSMAs but their transformation temperatures are at low technologically uninteresting temperatures. $\text{Fe}_{70}\text{Pd}_{30}$ alloys are MSMAs at slightly below room temperature²⁴ and other compositions have the potential of being engineered like FeNiCoTi.²⁵ FeMnSiX alloys are SMAs and potentially MSMAs, but, because of their large hysteresis they are limited in their usefulness.

SUMMARY

Martensites occur, among others, in Cu- and Fe-based alloys. Between those two, natural SMAs exist predominantly in the former systems. Binary bcc Cu-based alloys are vibrationally stabilized Hume–Rothery phases which transform martensitically in the vicinity of a critical s -electron/atom ratio. A Kohn anomaly appears to be involved in ternary Cu-based SMAs.²⁶ Natural Fe-based SMAs have

transformation temperatures far below ambient but can be engineered to become SMAs, and naturally MSMAs.

Heusler alloys form a class of materials forming natural MSMAs. Magnetically, they conform to the Slater–Pauling plot. The martensitic instability occurs at an ($s+d$) electron/atom ratio of 7.4 whose significance is unknown at this time. Known Heusler alloys in the vicinity of this ratio are listed in Table I, in which known MSMAs are shown in boldface. Table I suggests various stoichiometric alloys which could be MSMAs. Nonstoichiometric alloys and quaternary systems of the Heusler alloys listed in Table I might be MSMAs. However, little is known about those phase diagrams at this time.

ACKNOWLEDGMENTS

The work at the University of Maryland was supported by the Office of Naval Research, Contract No. N00015-99-1-08337, ONR/DARPA Contract No. N00014-95-1-1071, as well as the National Science Foundation, Grant No. DMR-97-06815. Cosmi Craciunescu's help with some of the figures was very much appreciated. The research at the University of Minnesota was supported by Contract Nos. ONR N00014-95-1-1145 and 99-1-0925. It also benefited from the support of ARO DA/DAAG55-98-1-0335, Grant No. NSF DMS-9505077, and Contract No. AFOSR/MURI F49620-98-1-0433.

¹M. Cohen, *Phase Transformations* (Wiley, New York, 1951), pp. 588–660.

²G. B. Olson, *Martensite* (ASM, Metals Park, OH, 1992), p. 1.

³W. C. Leslie, *The Physical Metallurgy of Steels* (McGraw-Hill, New York, 1981), p. 71.

⁴R. D. James and K. Hane, *Acta Mater.* (to be published).

⁵T. Maki, K. Kobayashi, M. Minato, and T. Tamura, *Scr. Mater.* **18**, 1105 (1984).

⁶C. Zener, *Phys. Rev.* **71**, 846 (1947).

⁷P. E. A. Turchi, M. Sluiter, F. J. Pinski, D. D. Johnson, Dn. M. Nicholson, G. M. Stocks, and J. B. Staunton, *Phys. Rev. Lett.* **67**, 1799 (1991).

⁸M. Schroeter, E. Hoffmann, M. S. Ynag, P. Entel, H. Akai, and A. Altrgge, *J. Phys. IV* **C8**, 273 (1995).

⁹S. M. Shapiro, B. X. Yang, Y. Noda, L. E. Tanner, and D. Schryvers, *Phys. Rev. B* **43**, 931 (1991).

¹⁰D. J. Gunton and G. A. Sanders, *Solid State Commun.* **14**, 865 (1974).

¹¹X. Ren, K. Taniwaki, K. Otsuka, T. Suzuki, K. Tanaka, Y. I. Chumlyakov, and T. Ueki, *Philos. Mag. A* **79**, 31 (1999).

¹²E. F. Wassermann and P. Entel, *J. Phys. IV* **C8**, 287 (1995).

¹³E. Hoffmann, H. Herper, P. Entel, S. G. Mishra, P. Mohn, and K. Schwarz, *Phys. Rev. B* **47**, 5589 (1993).

¹⁴G. Hausch, *J. Phys. Soc. Jpn.* **37**, 819 (1974); **37**, 824 (1974).

¹⁵S. Muto, R. Oshima, and F. E. Fujita, *Acta Metall. Mater.* **38**, 685 (1990).

¹⁶P. J. Webster, K. R. A. Ziebeck, S. L. Town, and M. S. Peak, *Philos. Mag. B* **49**, 295 (1984).

¹⁷I. K. Zasimchuk, V. V. Kokorin, V. V. Martynov, A. V. Tkachenko, and V. A. Chernenko, *Fiz. Met. Metalloved.* **6**, 110 (1990).

¹⁸V. V. Kokorin, V. A. Chernenko, E. Cesari, J. Pons, and C. Segui, *J. Phys.: Condens. Matter* **8**, 6457 (1996).

¹⁹A. Zheludev, S. M. Shapiro, P. Wochner, A. Schwartz, M. Wall, and L. E. Tanner, *J. Phys. IV* **C8**, 1139 (1995).

²⁰R. M. Bozorth, *Ferromagnetism* (IEEE, Piscataway, NJ, 1993), p. 441.

²¹V. A. Chernenko, E. Cesari, V. V. Kokorin, and I. N. Vitenko, *Scr. Metall. Mater.* **33**, 1239 (1995); A. N. Vasil'ev, A. D. Bozhko, V. V. Khovailo, V. D. Buchelnikov, M. Matsumoto, S. Suzuki, T. Takagi, and J. Tani, *Phys. Rev. B* **59**, 1113 (1999); F. Zuo, X. Su, P. Zhang, G. C. Alexandrakis, F. Yang, and K. H. Wu, *J. Phys.: Condens. Matter* **11**, 2821 (1999); K. Tsuchiya, A. Ohashi, H. Nakamura, and M. Umamoto, *International Conference on Solid-Solid Phase Transformations 1999, Kyoto, Japan*, edited by M. Koiwa, K. Otsuka, and T. Miyazaki (The Japan Institute of Metals, 1999), p. 1108. M. Wuttig and Y. Zheng (unpublished).

²²F. A. Hames and D. S. Eppelsheimer, *Nature (London)* **161**, 562 (1948).

²³M. Wuttig and Y. Zheng (unpublished).

²⁴R. D. James and M. Wuttig, *Philos. Mag. A* **77**, 1273 (1998).

²⁵M. Wuttig (unpublished).

²⁶E. F. Wassermann, J. Kaestner, M. Acet, and P. Entel, *International Conference on Solid-Solid Phase Transformations, 1999, Kyoto, Japan*, edited by M. Koiwa, K. Otsuka, and T. Miyazaki (The Japan Institute of Metals, 1999), p. 807.